

Risk assessment of agricultural water requirement based on a multi-model ensemble framework, southwest of Iran

Reza Zamani¹ · Ali-Mohammad Akhond-Ali¹ ·
Abbas Roozbahani² · Rouhollah Fattahi³

Received: 29 November 2015 / Accepted: 19 May 2016 / Published online: 1 June 2016
© Springer-Verlag Wien 2016

Abstract Water shortage and climate change are the most important issues of sustainable agricultural and water resources development. Given the importance of water availability in crop production, the present study focused on risk assessment of climate change impact on agricultural water requirement in southwest of Iran, under two emission scenarios (A2 and B1) for the future period (2025–2054). A multi-model ensemble framework based on mean observed temperature-precipitation (MOTP) method and a combined probabilistic approach Long Ashton Research Station-Weather Generator (LARS-WG) and change factor (CF) have been used for downscaling to manage the uncertainty of outputs of 14 general circulation models (GCMs). The results showed an increasing temperature in all months and irregular changes of precipitation (either increasing or decreasing) in the future period. In addition, the results of the calculated annual net water requirement for all crops affected by climate change indicated an increase between 4 and 10 %. Furthermore, an increasing process is also expected regarding to the required water demand volume. The most and the least expected increase in the water demand volume is about 13 and 5 % for A2 and B1 scenarios, respectively. Considering the results and the limited water resources in the study area, it is

crucial to provide water resources planning in order to reduce the negative effects of climate change. Therefore, the adaptation scenarios with the climate change related to crop pattern and water consumption should be taken into account.

1 Introduction

In recent years, changes in precipitation, temperature, and evaporation, which are key climatic variables, have had significant negative effects on agriculture due to climate change and global warming. Among the various water consumers, agriculture is very vulnerable to effects of climate change. Growing population, increasing demand, and diet change increase freshwater consumption in the future through irrigation agriculture to produce more food (Foley et al. 2011; UNESCO 2012; Wada and Bierkens 2014). Although, developing irrigation to increase food production has serious effects on the environment because of the limited freshwater availability (Reilly and Schimmelpfennig 1999). According to the Food and Agriculture Organization of the United Nations (FAO) (1999) and Postel (1999), the irrigated areas have increased as much as six times over the world. Similarly, 40 % of the world's food is produced from irrigated farms. On the other hand, the irrigated area has expanded 1 % per year, and based on Cai and Rosegrant (2002), the demand for irrigation will be increased almost 14 % by 2025. In dealing with areas with limited water resources area, decline in food productions has a direct effect on human life and increases poverty in the local scale (Olesen and Bindi 2002). Accordingly, increasing water security is very crucial in such areas, which is one of the sufficient ways of water management and sustainable development. In order to develop water management policies and sustainability of agriculture, it is essential to assess the impacts of climate change on agricultural water requirement.

✉ Reza Zamani
rzamani.am@gmail.com

¹ Department of Hydrology and Water Resources, Faculty of Water Sciences Engineering, Shahid Chamran University of Ahvaz, Ahvaz 6135783135, Iran

² Department of Irrigation and Drainage, College of Aburairhan, University of Tehran, Pakdasht, Tehran 3391653755, Iran

³ Department of Water Engineering, Faculty of Agriculture, Shahrekord University, Shahrekord, Iran

Recently, many investigations have been carried out in this sector (Garrote et al. 2015; Multsch et al. 2015 and Riediger et al. 2016). A study by Elgaali et al. (2007) showed climate change effects on irrigation water demand in southeastern Colorado. They found an increase in irrigation water demands under climate change. Rodríguez Díaz et al. (2007) studied the climate change impact on water requirement in Guadalquivir river basin in Spain. According to their report, there was a 15–20 % increase in irrigation water requirement in 2050. Using the decision support system for agro-technology transfer (DSSAT)-Canegro model, Knox et al. (2010) reported that climate change in the 2050s could increase sugarcane irrigation water requirements in Swaziland more than 9 %, and sucrose yields about 15 %. A study by Trnka et al. (2011) showed that there will be increased irrigation requirement due to climate change in the Central Mediterranean and the Iberian Peninsula for both winter and spring crops. Shahid (2011) analyzed the impacts of climate change on irrigation water demand of dry-season Boro rice in northwest Bangladesh. The results indicated that there will be no significant changes in total irrigation water requirement under climate change, while there will be an increased daily use of water for irrigation. Savé et al. (2012) studied irrigation water demand under climate change in a Spanish basin. They reported an increased irrigation water requirement related to the crop pattern in the study area between 40 and 250 % at the end of the twenty-first century. Also, Gondim et al. (2012) reported future increase in irrigation water requirement under climate change in the Jaguaribe River basin, Brazil. In addition, Rehana and Mujumdar (2013) reported an increased irrigation requirement by investigating the regional impacts of climate change on irrigation water demands for paddy, sugarcane, permanent gardens, and semidry crops over the command area of Bhadra reservoir, India. Elliott et al. (2014) found that the CO₂ effects on crop growth and transpiration are a significant source of uncertainty for the assessment of climate change impacts on crop yields. In another study, Lee and Huang (2014) studied changes in irrigation demand under climate change for the future period (2046–2065) and compared the results to the base period (2004–2011) in north of Taiwan. They reported some increases in temperature and precipitation, which consequently led to changes in effective rainfall and crop requirement. Their study suggested an insignificant difference (<2.5 %) between current and future irrigation water requirements. Ashofteh et al. (2014) investigated the effects of climate change on agricultural water demand by considering risk analysis in East Azerbaijan, Iran. The results of this study indicated that risk of changes in crop water requirement increased approximately 3, 17, and 33 % for 25, 50, and 75 % risk levels, respectively. Valverde et al. (2015) examined the effects of climate change on irrigated agriculture in Guadiana river basin, in the south of Portugal. The results showed that there was an increase in crop irrigation

requirement, particularly for maize, pasture, and orchards. Woznicki et al. (2015) studied irrigation demand under climate change by considering uncertainty and developing adaptation scenario in Kalamazoo River basin, southwest Michigan, USA. The results indicated an uncertainty in irrigation water requirement; also, a decrease in demand has been reported as a result of the delayed planting.

In addition to the importance of the climate change impacts on water resources and agriculture, it is essential to consider the uncertainty existing in this field. In the studies of the climate change, the general circulation model (GCM) output is a major source of uncertainty (Hawkins and Sutton 2009). Among the reasons behind this uncertainty, one can mention the lack of adequate knowledge in climate systems and computational limits in simulation of physical processes on small scales (Williams and Tselioudis 2007; Knutti and Hegerl 2008; Greasby and Sain 2011). In using the GCM output in the related studies, there are two general approaches including single GCMs (Jones and Thornton 2003; Guo et al. 2010; Teixeira et al. 2013; Ahmadi et al. 2015) and multi-model projection (Özdoğan 2011; Gohari et al. 2014). According to Lee et al. (2011) and Gohari et al. (2013), the first approach may cause an error in the estimation of climatic parameters. On the other hand, combined use of several climatic models helps to estimate a more reliable range of climate changes (Kloster et al. 2010). Accordingly, a multi-model ensemble of GCM outputs has been used in a large number of studies related to the effects of climate change on water resources and agriculture (e.g., Raje and Mujumdar 2010; Joyce et al. 2011; Zareian et al. 2014). Weighting method is one of the multi-model approaches that used to manage the uncertainty of GCM output (Tebaldi and Knutti 2007; Daccache et al. 2011). One type of weighting methods is the one based on the performance of the models in simulation of observed climatic parameters (Greene et al. 2006; Cai et al. 2009; Lee and Wang 2014), which is also based on a risk approach in this study.

In the present study, the effects of climate change on agricultural water requirement of network irrigation have been analyzed in Ramhormoz plain. A risk framework is used based on a multi-model ensemble of GCM output for a more sufficient management and better structuring of uncertainties. In this study, the full applied methodology covers two main stages: (a) risk assessment of climate change and (b) agricultural water demand calculation. The first stage includes (i) production of climate scenarios using 14 GCMs under two emission scenarios of A2 and B1; (ii) use of mean observed temperature-precipitation (MOTP) method for weighting GCMs, generation of discrete probability distribution functions (PDFs), developing cumulative distribution functions (CDFs), and then extracting probability percentiles (25, 50, and 75 %); and (iii) stochastic downscaling by using combined Long Ashton Research Station-Weather Generator (LARS-WG) and change factor (CF).

2 Material and methods

2.1 Case study

The study area is the irrigation network of Ramhormoz plain, which is about 22,470 ha located in southwest of Iran. In this plain, the average annual precipitation is about 310 mm, and the average annual temperature is about 26 °C. Recently, the Jarreh reservoir, with 261-MCM volume, has been constructed in outlet of Zard river basin to provide the agricultural water requirement in this plain. Zard river basin has an elevation of 324 to 3295 m above sea level, the length of main channel is about 70 km, and average slope is about 3 %. Agriculture is considered as a major and important job in the study area. The main crop pattern of this plain is wheat, corn, barley, and alfalfa. The crop pattern of plants and their area under cultivation are shown in Table 1, and Fig. 1 shows the location of the study area in Iran.

2.2 Assessment of climate change

2.2.1 Production of climate scenarios

As prominent models for simulating the effects of increasing greenhouse gas concentration on global climate system, GCMs are mathematical models that attempt to describe the full three-dimensional geometry of Earth’s climate system. Table 2 describes 14 GCMs in detail, which are employed in this study under two emission scenarios (A2 and B1), extracted from the Fourth Assessment Report (AR4) of Intergovernmental Panel on Climate Change (IPCC). Describing a very heterogeneous world, A2 storyline and scenario assume a world with a continuously increasing global population and a regionally oriented economic growth that is more fragmented and slower than the other emission

Table 1 Crop pattern and area under cultivation of each crop in the Ramhormoz network irrigation

Crop	Area under cultivation (%)	Area under cultivation (ha)
Wheat	26.88	5752.32
Barley	15.53	3323.42
Corn	15.44	3304.16
Alfalfa	8.74	1870.36
Clover	9.37	2005.18
Bean	8	1712
Other crops ^a	21.04	4502.56
Total	105	22,470

^a Other crops according to the percent of total cultivation area include rice, soybean, watermelon, vegetable, cotton, sesame, citrus, and date, respectively

scenarios. The B1 storyline and scenario assume a convergent world with a global population that reaches to a peak in mid-century and thereafter declines. It assumes rapid changes in structures of economic toward a service and information economy with reductions in intensity of material and the introduction of clean and resource-efficient technologies (IPCC 2007).

2.2.2 MOTP method and probabilistic assessment

In this step, after extracting monthly climatic variables from GCMs under A2 and B1 scenarios, difference and relativity of long-term monthly average values of temperature and precipitation for the base period (1971–2000) were compared with the future period (2025–2054) using the following structure:

$$\Delta T_i = (\bar{T}_{GCM,fut_i} - \bar{T}_{GCM,base_i}) \tag{1}$$

$$\Delta P_i = \left(\frac{\bar{P}_{GCM,fut_i}}{\bar{P}_{GCM,base_i}} \right) \tag{2}$$

where ΔT_i and ΔP_i are average long-term monthly temperature and precipitation change for i^{th} month, respectively. \bar{T}_{GCM,fut_i} and \bar{P}_{GCM,fut_i} are average long-term monthly temperature and precipitation for i^{th} month, simulated by GCM under related scenario in future period, respectively. $\bar{T}_{GCM,base_i}$ and $\bar{P}_{GCM,base_i}$ represent average long-term monthly temperature and precipitation for i^{th} month, simulated by GCM in baseline period, respectively. This approach has been applied by Wilby and Harris (2006), Morid and Bavani (2010), and Zareian et al. (2014).

In the next step, to weigh each of the 14 GCMs, mean observed temperature–precipitation (MOTP) method is used based on Eq. (3). The most important feature of this method is considering the ability of the models to simulate the observed climate variables, i.e., the difference between the simulated long-term variables in each month in the baseline period and the corresponding observed values.

$$W_{ij} = \frac{\left(\frac{1}{\Delta d_{ij}} \right)}{\sum_{j=1}^{14} \left(\frac{1}{\Delta d_{ij}} \right)} \tag{3}$$

where W_{ij} is the weight of j^{th} GCM in i^{th} month and Δd_{ij} is the difference between average temperature or precipitation simulated by j^{th} GCM in i^{th} month of base period and the corresponding observed value (Gohari et al. 2013).

In the following, monthly temperatures and relative changes of precipitation with the weights of corresponding GCMs were used to construction of PDFs for each month. Based on the prototype of discrete PDFs and similar studies (Pindyck 2012; Teutschbein and Seibert 2012; Gohari et al. 2013),

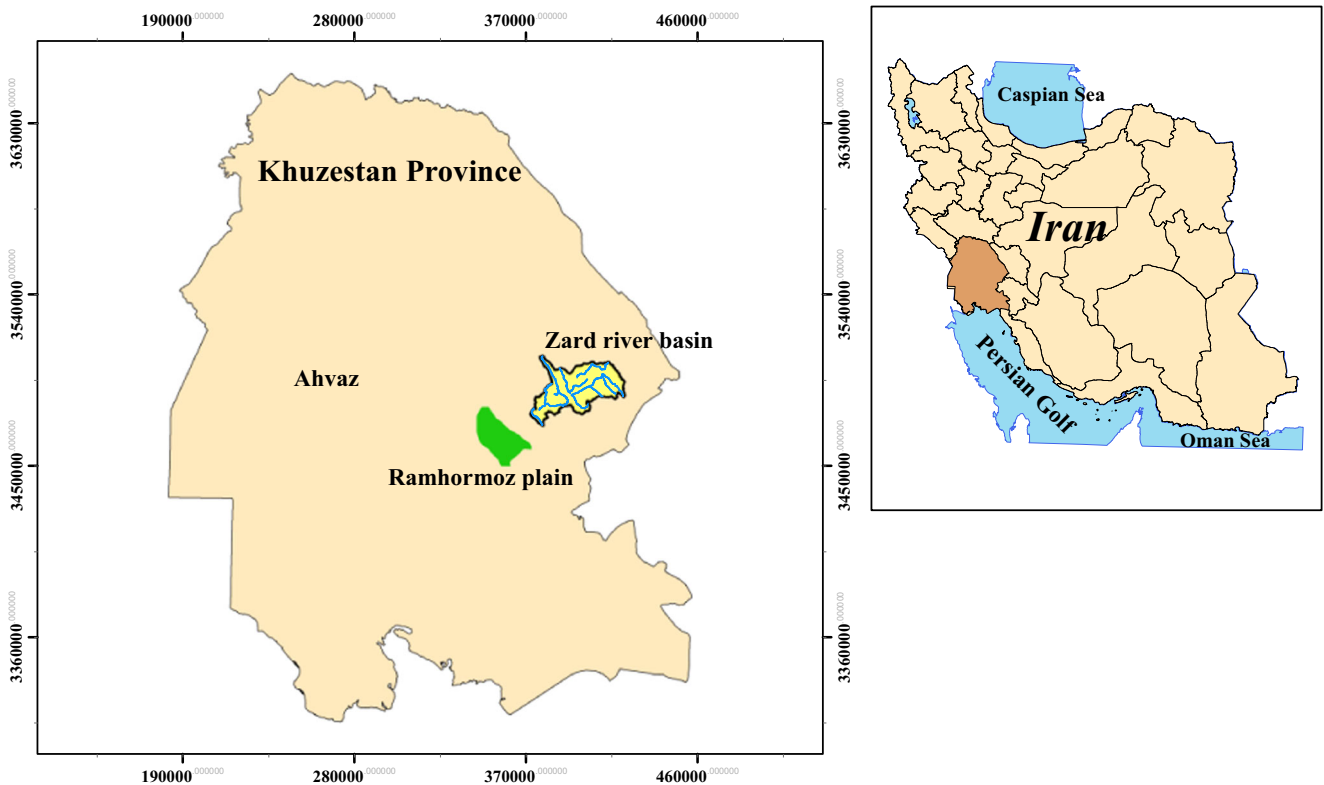


Fig. 1 Location of the study area in Iran

Gamma distribution with two parameters has been chosen to construct continuous distributions as follows:

$$f(x) = \frac{1}{\Gamma(k)b^k} x^{k-1} e^{-x/b}; \quad x \geq 0 \quad (4)$$

$$\Gamma(k) = \int_0^\infty x^{k-1} e^{-x} dx \quad (5)$$

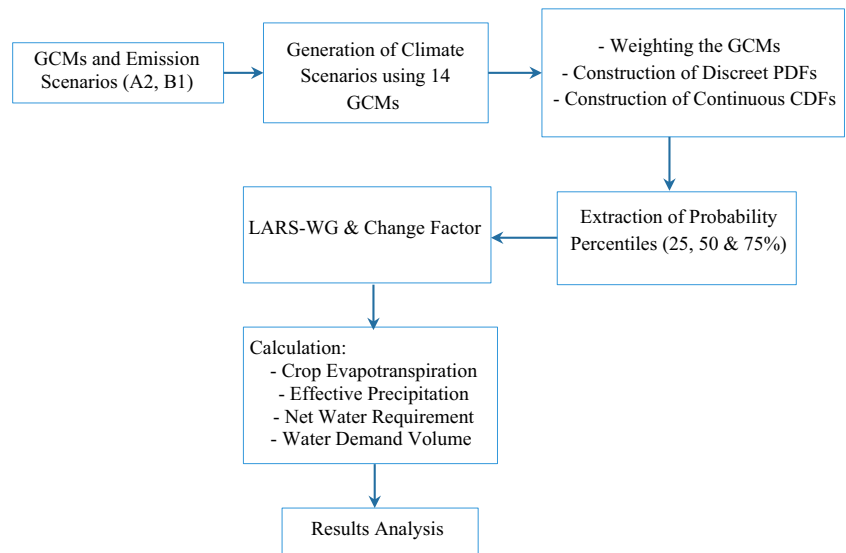
where x is the variable, k and b are shape and scale parameters, and $\Gamma(k)$ equals the incomplete Gamma function. It should be mentioned that the values of k and b are changed to get the best fit based on the maximum likelihood estimation method using sum of squared error (SSE), which functions as follows:

$$SSE = \sum_{i=1}^n (y_i - y_i^*)^2 \quad (6)$$

Table 2 Description of the GCMs from IPCC's Fourth Assessment Report (AR4)

Model	Center acronym	Resolution (degree)	Reference
BCM2	BCCR (Norway)	1.9 × 1.9	Déqué et al. (1994)
CGCM3 (T63)	CCCma (Canada)	1.9 × 1.9	McFarlane et al. (1992); Flato (2005)
CNRM-CM3	CNRM (France)	1.9 × 1.9	Déqué et al. (1994)
CSIRO-MK3	CSIRO (Australia)	1.9 × 1.9	Gordon et al. (2002)
ECHAM5-OM	MPI-M (Germany)	1.9 × 1.9	Roeckner et al. (2003)
ECHO-G	MIUB (Germany)	3.9 × 3.9	Roeckner et al. (1996)
GFDL-CM2	GFDL (USA)	2 × 2.5	Delworth et al. (2006)
GISS-E-R	GISS (USA)	4 × 5	Schmidt et al. (2006)
HadCM3	UKMO (UK)	2.5 × 3.75	Gordon et al. (2000)
INM-CM3	INM (Russia)	4 × 5	Galini et al. (2003)
IPSL-CM4	IPSL (France)	2.5 × 3.75	Hourdin et al. (2006)
MRI-CGCM2.3.2	MRI (Japan)	2.8 × 2.8	Shibata et al. (1999)
CCSM3	NCAR (USA)	1.4 × 1.4	Collins et al. (2006)
PCM	NCAR (USA)	2.8 × 2.8	Kiehl et al. (1998)

Fig. 2 Flowchart of the methodology



where y_i is the data point, y_i^* is the estimation of gamma function, and n is the number of data points.

Accordingly, the developed discrete PDFs are used to construction of CDFs. More details about this method can be found in Gohari et al. (2013). In the next step, three different probabilistic scenarios are produced at three different percentiles (25, 50, and 75 %). The probability percentile represents low changes in temperature called “ideal scenario (IS)” and high changes in temperature called “critical scenario (CS),” and the probability percentile represents moderate changes in temperature called “moderate scenario (MS).”

2.2.3 Stochastic downscaling

As a downscaling technique, stochastic weather generator (WG) is used to produce daily site-specific climate scenarios (Barrow and Semenov 1995; Semenov 2007).

These models are able to simulate synthetic time series of daily weather, which are statistically similar to observed weather (Richardson and Wright 1984 and Semenov 2007). In the present study, daily time series has been generated by LARS-WG (Semenov and Barrow 2002) from monthly climate change scenarios and historical daily climate data. The best distribution function for the observed daily time series for baseline period (1971–2000) has been selected, and then, synthetic future (2025–2054) daily time series are have been generated by LARS-WG based on the extracted climate change scenarios for 25, 50, and 75 % probability percentiles under A2 and B1 emission scenarios. As well as, the model was run to generate 300 years of future daily time series for each climate change probability percentile so as to deal with uncertainty in the outputs of LARS-WG. Accordingly, through averaging, the 300-year time series was divided into ten plausible daily time series for a 30-year period, and then, the average daily values of these ten time series

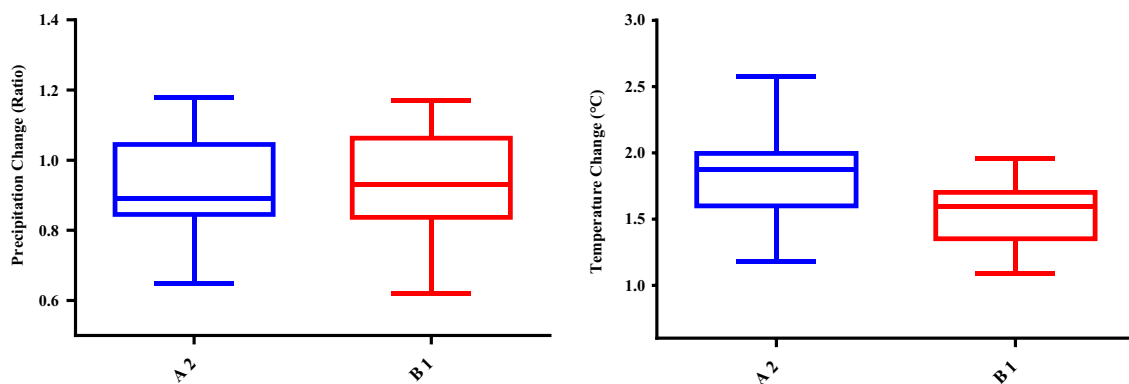


Fig. 3 Box plots of average annual precipitation and temperature changes under emission scenarios (2025–2054)

Table 3 Weights (%) for 14 GCMs of precipitation simulation in the base period

	Jan	Feb	Mar	Apr	May	Jun	Jul	Aug	Sep	Oct	Nov	Dec
BCM2	7.13	7.38	6.67	34.83	2.60	0.40	1.10	48.09	10.11	1.73	10.94	7.61
CGCM3 (T 63)	7.87	7.68	8.52	11.20	0.95	0.49	3.63	4.55	8.20	0.77	6.34	8.06
CNRM-CM3	7.24	7.66	8.11	4.12	1.01	0.07	0.74	0.68	1.48	72.84	4.78	6.86
CSIRO-MK3	7.57	6.89	6.82	6.78	15.05	1.63	10.48	3.50	5.05	1.86	5.58	7.24
ECHAM5-OM	7.31	6.74	7.48	2.01	4.06	30.76	13.59	3.67	5.81	1.08	5.30	7.09
ECHO-G	6.48	6.48	6.37	2.10	26.73	1.01	15.33	3.76	15.88	3.42	4.45	6.15
GFDL-CM2	6.66	7.50	7.45	7.92	13.22	29.09	8.96	3.53	11.08	1.89	4.80	6.39
GISS-E-R	6.44	6.20	5.96	1.53	4.81	7.35	10.98	3.56	5.05	0.93	3.94	6.03
HadCM3	9.28	10.09	9.23	18.17	2.68	1.16	10.14	3.50	5.27	1.53	31.79	11.23
INM-CM3	6.33	6.30	6.39	2.17	3.46	0.39	1.58	6.39	1.72	7.97	4.07	6.17
IPSL-CM4	6.85	6.67	6.77	2.03	11.23	1.68	9.12	3.48	5.15	0.92	4.01	6.26
MRI-CGCM2.3.2	7.12	7.34	7.75	3.37	0.95	0.56	1.81	9.88	5.88	2.25	5.09	7.07
CCSM3	7.43	6.89	6.59	1.91	8.08	2.23	2.82	1.87	14.03	2.05	5.02	7.40
PCM	6.30	6.18	5.89	1.84	5.17	23.20	9.72	3.53	5.28	0.74	3.89	6.44

are calculated. This approach was used by Gohari et al. (2013) to cut down the uncertainty of WG in generated climatic variables.

2.3 Agricultural water demand calculation

2.3.1 Crop evapotranspiration and effective precipitation calculation

Crop water requirement calculation is an important sector in agricultural water management. The FAO-24 methodology (Doorenbos and Pruitt 1977) is considered as the standard

method for crop water requirement calculation and has been used in this study as follows:

$$ET_{C_{j,t}} = K_{C_{j,t}} \times ET_{0,t} \tag{7}$$

where $K_{C_{j,t}}$ is the coefficient of the j^{th} crop in the t^{th} month, $ET_{0,t}$ is the reference crop evapotranspiration in the t^{th} month, and $ET_{C_{j,t}}$ represents evapotranspiration for the j^{th} crop in t^{th} month. The input parameters for Eq. (7) are the length of four individual stages (initial season, growth season, mid-season, and late season) during the growing season and related crop coefficients (Kc). These coefficients are defined as the ratio between ET_0 and ET_c for each part of the growing season (Multsch et al.

Table 4 Weights (%) for 14 GCMs of temperature simulation in the base period

	Jan	Feb	Mar	Apr	May	Jun	Jul	Aug	Sep	Oct	Nov	Dec
BCM2	0.22	2.62	2.69	3.22	2.85	0.69	1.92	1.61	1.02	2.82	1.64	3.29
CGCM3 (T 63)	0.22	2.79	2.32	2.59	2.63	0.71	1.94	1.62	0.98	2.66	1.54	3.08
CNRM-CM3	0.21	2.97	3.36	3.65	3.66	0.83	2.34	1.82	1.23	2.98	1.60	2.98
CSIRO-MK3	0.50	7.27	9.04	6.67	6.04	2.05	4.39	3.75	1.87	5.10	2.90	6.03
ECHAM5-OM	0.63	8.94	17.36	20.26	27.40	53.76	32.08	26.34	21.80	20.42	7.07	8.50
ECHO-G	0.48	6.55	8.05	8.42	7.08	2.00	4.83	4.60	3.05	9.12	4.65	7.18
GFDL-CM2	0.59	8.18	13.17	9.82	9.15	4.72	20.46	7.29	23.65	13.76	4.15	7.37
GISS-E-R	94.86	31.00	9.69	10.16	5.39	0.59	1.33	0.98	0.98	5.53	58.52	29.68
HadCM3	0.32	4.29	4.41	4.43	4.55	1.67	4.59	4.49	2.31	5.36	2.26	4.29
INM-CM3	0.34	4.11	3.62	3.38	2.85	0.51	1.16	1.01	0.78	2.66	1.88	4.20
IPSL-CM4	0.42	5.56	5.95	6.33	5.90	1.58	5.33	13.83	4.75	8.33	4.32	6.67
MRI-CGCM2.3.2	0.46	6.34	10.27	10.19	8.85	25.15	7.04	4.25	31.12	9.31	3.73	6.03
CCSM3	0.53	6.51	7.37	8.04	11.07	5.24	11.33	27.34	5.63	9.50	4.24	7.49
PCM	0.22	2.88	2.69	2.85	2.58	0.51	1.25	1.08	0.83	2.43	1.49	3.19

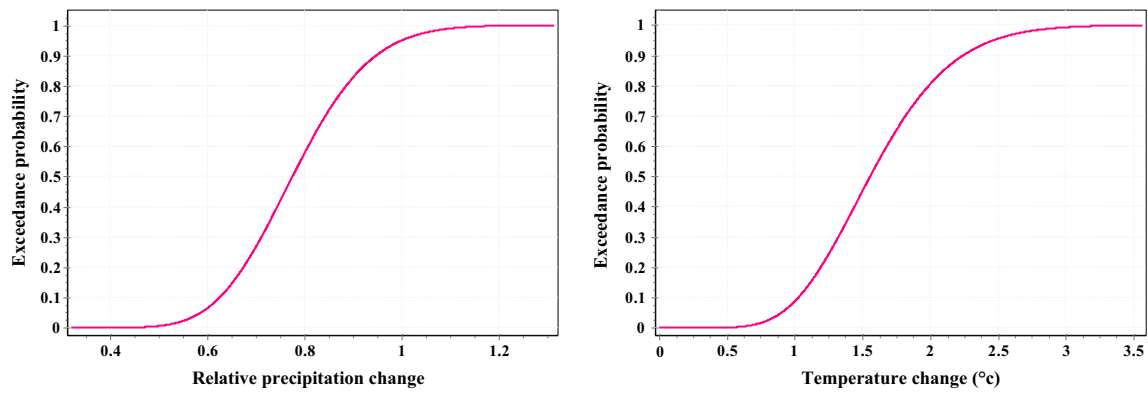


Fig. 4 Constructed CDFs for relative precipitation and temperature changes (Mar)

2015). Similarly, reference crop evapotranspiration can be derived based on the FAO Penman-Monteith method:

$$ET_0 = \frac{0.408 \Delta (R_n - G) + \gamma \frac{900}{T + 273} u_2 (e_s - e_a)}{\Delta + \gamma (1 + 0.34 u_2)} \quad (8)$$

where ET_0 = reference evaporation [mm day^{-1}], R_n = net radiation at the crop surface [$\text{MJ m}^{-2} \text{day}^{-1}$], G = soil heat flux density [$\text{MJ m}^{-2} \text{day}^{-1}$], T = mean daily air temperature at 2-m height [$^{\circ}\text{C}$], u_2 = wind speed at 2-m height [m s^{-1}],

e_s = saturation vapor pressure [kPa], e_a = actual vapor pressure [kPa], $e_s - e_a$ = saturation vapor pressure deficit [kPa], Δ = slope vapor pressure curve [$\text{kPa } ^{\circ}\text{C}^{-1}$], and γ = psychrometric constant [$\text{kPa } ^{\circ}\text{C}^{-1}$].

In this study, the USDA Soil Conservation Service (SCS) method has been employed to calculate effective rainfall using the CROPWAT model (Smith 1992; Clarke et al. 2000) based on the following:

$$PE_{\text{eff}} = \frac{P_{\text{tot}}(125 - 0.2P_{\text{tot}})}{125} \quad \text{for } P_{\text{tot}} \leq 250 \text{mm} \quad (9)$$

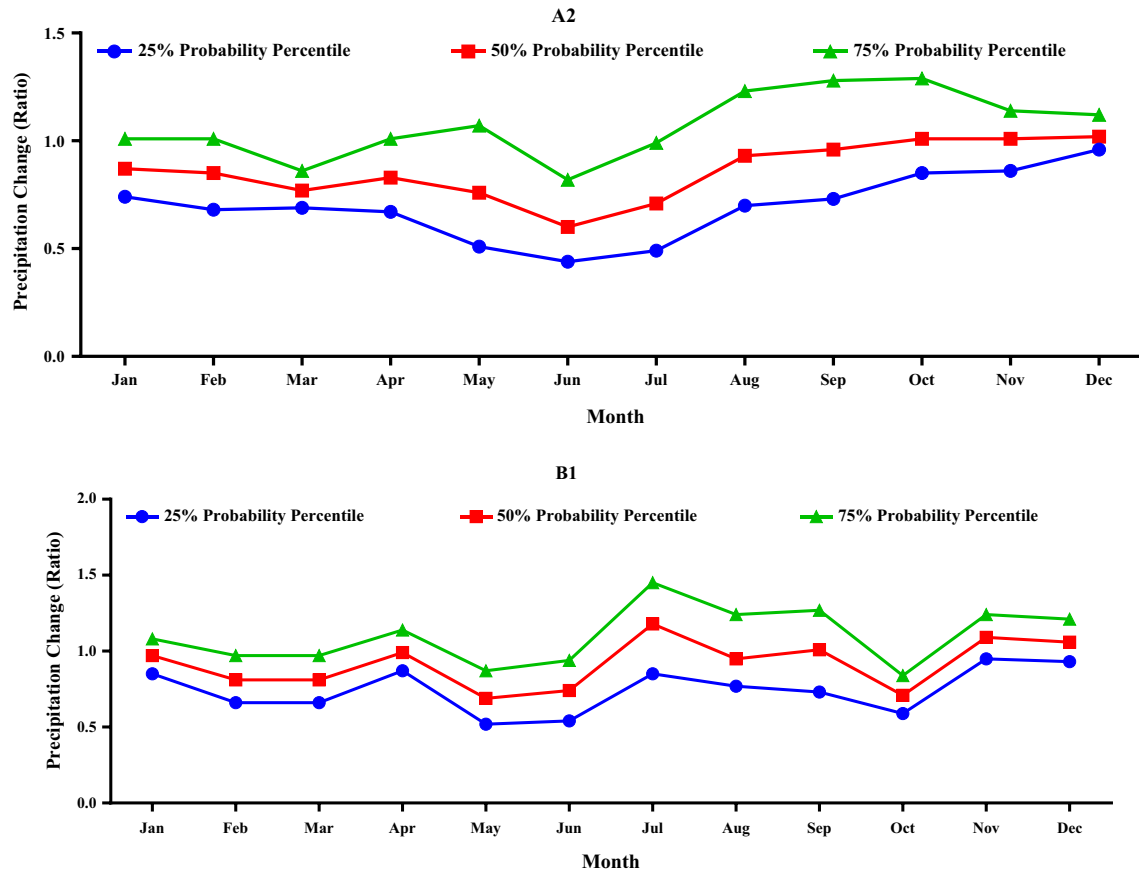


Fig. 5 Monthly expected precipitation changes (ratio) at different probability levels under emission scenarios (2025–2054)

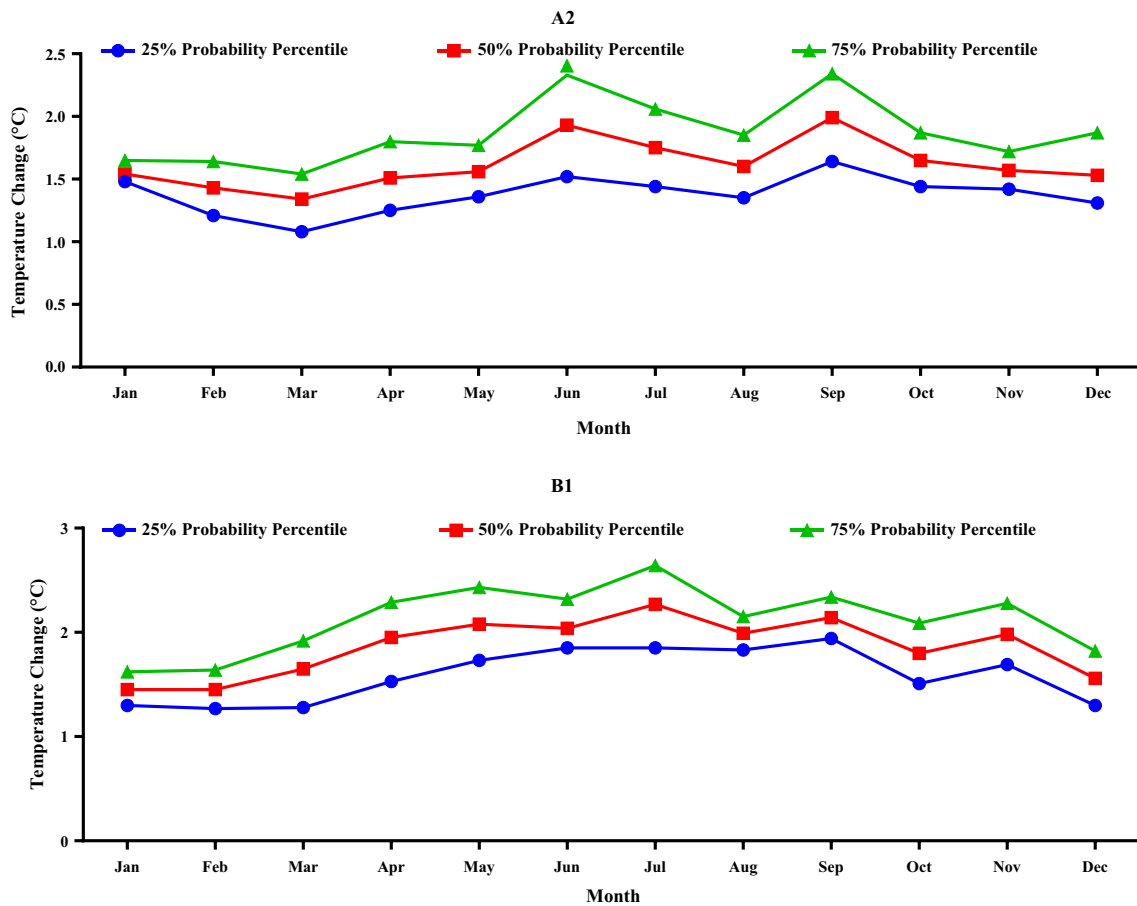


Fig. 6 Monthly expected temperature changes (°C) at different probability levels under emission scenarios (2025–2054)

$$PE_{eff} = 125 + 0.1P_{tot} \quad \text{for } P_{tot} > 250^{mm} \quad (10)$$

where PE_{eff} is the effective precipitation (mm) and P_{tot} represents total precipitation (mm).

2.3.2 Net water requirement and water demand volume estimation

Following the previous steps, the net water requirement and water demand volume are calculated based on Eqs.(11) and (12), respectively (Ashofteh et al. 2013; Multsch et al. 2015).

$$NWR_{t,j} = \max(ET_{c,t,j} - PE_{eff,t}, 0) \quad (11)$$

$$WDV_{t,j} = \left(\frac{NWR_{t,j} \times A_j}{100,000} \right) \quad (12)$$

where $NWR_{t,j}$ is the net water requirement (mm) for the j^{th} crop in t^{th} month, $WDV_{t,j}$ is the water demand volume ($\times 10^6 \text{ m}^3$) for the j^{th} crop in t^{th} month, and A_j equals the area under cultivation (ha) for j^{th} crop. The steps that are mentioned above are shown in Fig. 2.

3 Results and discussion

The box plots of changes of average annual precipitation and temperature in the study area, which are outputs from 14

Table 5 Seasonal and annual downscaled variable changes at different probability levels under emission scenarios (2025–2054)

	A2			B1		
	25 %	50 %	75 %	25 %	50 %	75 %
Temperature change (°C)						
Winter	0.74	0.85	1.10	0.73	0.86	1.02
Spring	0.71	1.10	1.25	0.50	0.70	0.88
Summer	1.69	1.99	2.00	1.39	1.63	1.87
Autumn	1.96	2.13	2.33	1.80	1.97	2.15
Annual	1.28	1.50	1.67	1.10	1.29	1.48
Precipitation change (%)						
Winter	-12.34	-3.89	0.57	-12.33	-1.31	2.12
Spring	-16.69	-7.89	-4.67	-16.00	-6.65	-3.24
Summer	6.76	10.93	16.39	14.79	13.18	15.99
Autumn	4.48	9.66	17.14	3.26	12.48	17.32
Annual	-10.73	-2.70	1.94	-10.75	-0.38	3.27

Table 6 Annual ET_c (mm) at different probability levels under emission scenarios (2025–2054)

Crops	His	A2			B1		
		CS	MS	IS	CS	MS	IS
Wheat	501.66	606.28	578.18	564.12	574.12	556.25	541.81
Barley	280.30	370.80	343.99	331.16	342.73	325.81	312.44
Corn	527.80	563.55	554.57	553.93	552.20	545.42	542.99
Alfalfa	1754.84	1885.49	1855.01	1841.78	1847.45	1821.19	1814.74
Clover	665.23	835.93	785.01	749.67	786.80	756.47	718.31
Bean	116.87	196.34	172.07	162.55	172.29	159.52	149.24
Other crops	6805.69	7276.08	7160.88	7112.18	7156.25	7053.34	7015.83

GCMs [extracted from the data distribution center of IPCC (DDC: <http://www.ipcc-data.org>)], are shown in Fig. 3 for the future period (2025–2054) under two emission scenarios (A2 and B1). Based on the results, changes in average annual precipitation under A2 scenario range from 35 % decrease to 15 % increase, which can be changeable, and results of B2 scenario depicted a range from 37 % decrease to 18 % increase for the future period compared to the base period. Unlike this expected irregular process in precipitation changes, there is an expected regular increase of more than 1 °C in average annual temperature in all GCMs. The increasing rate of temperature between the two scenarios is different, and more increase is expected under A2 scenario. The highest increase of average annual simulated temperature by GCMs is 2.58 °C under scenario A2, and the least increase is 1.18 °C. The values under B1 scenario are 1.95 and 1.09 °C, respectively. In the outputs of all models, an increasing trend is seen in simulated temperature for future period compared to base period. According to these results, an uncertainty in simulation and outputs of different GCMs is clearly shown.

In the present study, the MOTP method of GCMs has been used in order to decrease the effects of this uncertainty. The results gained from GCM weight giving in simulated precipitation and temperatures in the base period are shown in Tables 3 and 4. The models HadCM3 and ECHO-G have the best performance (most weight) in simulated precipitation in the base period. Similarly, the models GISS-ER and

ECHAM5-OM have the highest weight in simulating temperature in the base period. After weighting GCMs, the discrete PDFs and CDFs of monthly precipitation and temperature have been developed, as shown in Fig. 4.

Figures 5 and 6 show monthly precipitation and temperature changes at different probability levels of 25, 50, and 75 % under emission scenarios (A2, B1). The change amount of monthly temperature under both scenarios is increasing in all months. This increasing amount of temperature differs in different months. Based on the results, the increases of expected average annual temperature under A2 scenario for probability levels of 75, 50, and 25 % were equal to 2.09, 1.89, and 1.59 °C, respectively, and 1.88, 1.61, and 1.36 °C for B1 scenario. It can be concluded that under A2 scenario, more increase in temperature is expected. Also, precipitation under climate change is expected to be very changeable and irregular under both scenarios, and most of the changes are observed in August and September. For example, at the probability level of 75 % under A2 scenario, the changes are observed with the ratios of 1.43 and 1.28 in August and September compared to changes in June with a ratio of 0.79. For B1 scenario, the ratio of changes has been from 1.45 in July to 0.84 in October at the probability level of 75 %.

After evaluating and checking the performance of LARC-WG model in the study area, the expected monthly changes of temperature (minimum and maximum) and precipitation at different probability levels are downscaled for 300-year time

Table 7 Annual NWR (mm) at different probability levels under emission scenarios (2025–2054)

Crops	His	A2			B1		
		CS	MS	IS	CS	MS	IS
Wheat	766.86	830.48	826.08	822.42	809.42	806.45	803.61
Barley	540.41	592.80	589.39	586.86	576.13	573.81	571.74
Corn	589.10	616.35	613.67	610.43	605.50	603.32	600.69
Alfalfa	2018.71	2131.29	2125.31	2115.32	2104.15	2096.19	2087.92
Clover	1169.16	1274.46	1266.97	1260.58	1239.00	1233.94	1228.93
Bean	361.08	401.84	399.27	397.65	389.59	387.91	386.46
Other crops	7800.26	8214.79	8194.51	8156.24	8121.27	8090.12	8057.79

Table 8 Annual WDV ($\times 10^6 \text{ m}^3$) at different probability levels under emission scenarios (2025–2054)

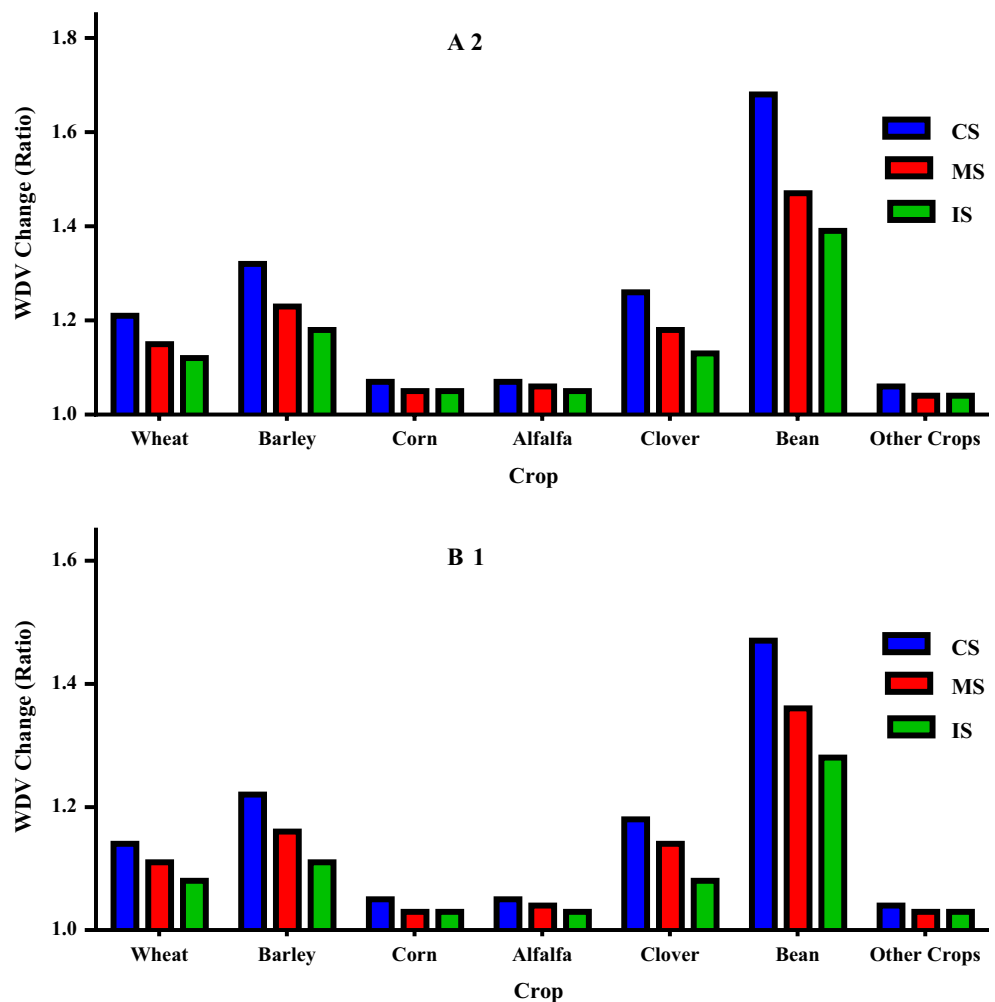
Crops	His	A2			B1		
		CS	MS	IS	CS	MS	IS
Wheat	28.86	34.88	33.26	32.45	33.03	32.00	31.17
Barley	9.32	12.32	11.43	11.01	11.39	10.83	10.38
Corn	17.44	18.62	18.32	18.30	18.25	18.02	17.94
Alfalfa	32.82	35.27	34.70	34.45	34.55	34.06	33.94
Clover	6.67	8.38	7.87	7.52	7.89	7.58	7.20
Bean	2.00	3.36	2.95	2.78	2.95	2.73	2.56
Other crops	36.98	39.08	38.60	38.45	38.59	38.11	38.00

series. In the next step, the series of 300 years are broken to 30-year time series, and finally, the daily average of these series is calculated. The seasonal and annual climatic variable changes are shown in Table 5, which were downscaled at probability levels of 25, 50, and 75 %. Based on the results, the increasing rates of seasonal and annual average temperature under A2 scenario are more than those under B1 scenario.

The highest increase in temperature is expected in autumn and summer. In addition, the precipitation changes differ in seasons and it can be, in some way, expected to observe a decrease in average precipitation in spring and summer under both scenarios. Also, the most expected decrease of mean annual and seasonal (spring) precipitation was predicted to occur at the probability level of 25 %.

Accordingly, the monthly averages at probability scenarios of CS, MS, and IS have been used to estimate the amount of ET_0 in the future period. In all months, the results show an increase in ET_0 . The most significant increase of ET_0 is expected under A2-CS belonging to March and August. Considering the amount of different K_C in each month, which is related to each crop based on the FAO journal, local studies, experiences, and growth periods for each crop (supposing the area under cultivation for each crop is unchangeable), the amount of ET_c has been calculated in different months affected by climate change. The results of calculated annual ET_c under climate change using probability scenarios are shown in Table 6. Results indicated an increase in ET_c in future period compared to the base period. This increase under A2

Fig. 7 Annual WDV changes (ratio) at different probability levels under emission scenarios (2025–2054)



scenario is expected to be more than B1's, which, compared to the higher increase in simulated temperature, seems natural. Also, the increase in ET_c at probability scenarios of CS is more than that of MS and IS. After calculating the effective precipitation based on the Eqs. (9) and (10), net water requirement and water demand volume are calculated for the future period, which are shown in Tables 7 and 8. Under both emission scenarios in the amount of water required for all crops, an increase is expected in all three probability scenarios. The amount of annual net water requirement for crops in irrigation network has increased approximately 10, 7, and 6 % for probability scenarios of CS, MS, and IS under emission scenario of A2. The numbers for B1 scenario are equal to 7, 5, and 4 %. The highest changes of net water requirement increase are expected to be for the crops of bean, barley, clover, and wheat. The ratio of changes in annual net water requirement in the period of 2025–2054 compared to the base period for these crops is 1.68, 1.32, 1.26, and 1.21, respectively.

Table 8 shows the results gained through calculating the water demand volume in the future period compared to the base period. Considering the area under cultivation, the most increase in water demand volume in the future period is expected to be for wheat, barley, and alfalfa. The amounts of annual changes in expected water demand volume for all crops in future period compared to the base period under A2 scenario for probability scenarios of CS, MS, and IS are 17.82, 13.04, and 10.84 ($\times 10^6$ m³). These numbers are, respectively, 12.56, 9.25, and 7.11 ($\times 10^6$ m³) for that under B1 scenario. The ratios of annual water demand volume for specified crops under emission scenarios of A2 and B1 are shown in Fig. 7. Based on the results, at CS and under both A2 and B1 scenarios, the most significant changes are seen in ratio of water demand volume for plants. The most meaningful changes in CS are for bean, barley, and clover, with ratios of 1.67, 1.32, and 1.26, respectively. In this regard, the values of B1 scenario are 1.47, 1.22, and 1.18, respectively.

Generally, results showed an increase in water demand volume in future period compared to the base period, which could cause problems in agriculture management and food provision security of the study area considering the dry and semi-dry climates of this region and limited water resources. In addition, on results of the changes in climatic variables that caused an increase in irrigation water requirement, runoff from the Zard basin and Jarreh reservoir inflow quantity will surely be changed as well. Therefore, applying an adaptive management in water resources systems can be used as alternative solution for declining system vulnerability in the studied area.

4 Conclusion

Considering the impacts of agriculture on human life, an investigation of the effects of climate change on agriculture can

better help water management and sustainable development. This issue seems to be more crucial in dry and semi-dry regions like Iran. Accordingly, in the present study, the effects of climate change on agricultural water requirement under different probability levels in Ramhormoz plain in southwest of Iran have been investigated. A risk framework has been used to manage uncertainties of GCM output and emission scenarios. In this framework, 14 GCMs are used under two emission scenarios of B1 and A2 through the MPOT method and a probabilistic approach. This methodology can be a proper solution to manage the uncertainty caused by the usage of GCMs in the assessment of climate change studies. The other aspects of uncertainty in irrigation demand under climate change are suggested to be addressed in future studies.

The results of examining the changes in monthly temperature indicated an increasing trend in all months and under both emission scenarios. Unlike the increasing and regular changes of temperature in the study area, an irregular change in precipitation (either decreasing or increasing) is expected in the future period compared to the base period. In addition, results of downscaled temperature under probability scenarios of CS, MS, and IS using LARS-WG model indicated an increase approximate to 1.67, 1.5, and 1.28 °C for A2 scenario and 1.48, 1.29, and 1.1 °C for B1 scenario, respectively, for the average annual temperature of the future period (2025–2054). It should be noted that the most expected decrease in precipitations under the studied emission scenarios is attributed to the probability scenario of CS with a value of approximately 10 %.

Calculation results related to ET_c showed a monthly increase under both emission scenarios, as well as an increase in the amount of net water requirement and water demand volume. The increase in water demand volume and expected net water requirement in CS under both emission scenarios (A2, B1) is higher compared to the other probability scenarios (MS and IS) and shows a more severe condition. The amounts of expected increase of water requirement for probability scenarios of CS, MS, and IS are equal to 1082, 797, and 663 mm under emission scenario of A2 and 780, 565, and 443 mm for B1 scenario, respectively. Regarding to the area under cultivation for each crop, the increasing amounts of annual water demand volume in the study area in probability scenarios of CS, MS, and IS are 13, 10, and 8 % under A2 scenario and 9, 7, and 5 % under B1 scenario, respectively. This increasing amount in A2 scenario, considering its critical assumptions, is more than B1 scenario. Similarly, an increase in irrigation demand under climate change has been reported by Fischer et al. (2007), Gohari et al. (2013), Ashofteh et al. (2014), and Riediger et al. (2016).

Technical studies of climate change impacts on local-regional polices such as the construction of dams and hydraulic structures are very important. These strategies can enhance the performance of water resources systems and reduce the

negative effects of climate change in the future. For example, according to the reports of Khuzestan water and power consulting, the construction studies of Abolabbas dam located upstream of the Jarreh reservoir (as a source of water supply to Ramhormoz plain) and Abolfares dam on A'alla river (as the other source of water supply) are currently under study. Therefore, an increase in net water requirement and water demand volume for the studied area (Ramhormoz plain) as was concluded in the present study can be useful for planning of these projects, and the authors suggest to consider this issue in the related studies.

Finally, given the limited water resources in dry and semi-dry regions like Iran and the role of agriculture in Iran's economy, the development of adaptation scenario policies such as reduction of water loss, improving the efficiency of irrigation system, optimal irrigation planning, enhancing water use efficiency, applying the water price policies, changes in cropping patterns, etc. can reduce vulnerability in this sector.

References

- Ahmadi M, Haddad OB, Loáiciga HA (2015) Adaptive reservoir operation rules under climatic change. *Water Resour Manag* 29:1247–1266
- Ashofteh PS, Haddad OB, Mariño MA (2013) Climate change impact on reservoir performance indexes in agricultural water supply. *J Irrig Drain Eng* 139:85–97. doi:10.1061/(ASCE)IR.1943-4774.0000496
- Ashofteh P, Haddad OB, Mariño MA (2014) Risk analysis of water demand for agricultural crops under climate change. *J Hydrol Eng* 20: 4014060. doi:10.1061/(ASCE)HE.1943-5584.0001053
- Barrow EM, Semenov MA (1995) Climate change scenarios with high spatial and temporal resolution for agricultural applications. *Forestry* 68:349–360. doi:10.1093/forestry/68.4.349
- Cai X, Rosegrant MW (2002) Global water demand and supply projections. *Water Int* 27:159–169. doi:10.1080/02508060208686989
- Cai X, Wang D, Zhu T, Ringler C (2009) Assessing the regional variability of GCM simulations. *Geophys Res Lett.* doi:10.1029/2008GL036443
- Clarke D, Smith M, El-Askari K (2000) *CropWat for windows: user guide*. FAO, Roma
- Collins WD, Bitz CM, Blackmon ML, Bonan GB, Bretherton CS, Carton JA, et al. (2006) The community climate system model version 3 (CCSM3). *J Clim* 19:2122–2143. doi:10.1175/JCLI3761.1
- Daccache A, Weatherhead EK, Stalham MA, Knox JW (2011) Impacts of climate change on irrigated potato production in a humid climate. *Agric For Meteorol* 151:1641–53
- Delworth TL, Broccoli AJ, Rosati A, et al. (2006) GFDL's CM2 global coupled climate models. Part I: formulation and simulation characteristics. *J Clim* 19:643–674. doi:10.1175/JCLI3629.1
- Déqué M, Dreveton C, Braun A, Cariolle D (1994) The ARPEGE/IFS atmosphere model: a contribution to the French community climate modelling. *Clim Dyn* 10:249–266. doi:10.1007/BF00208992
- Doorenbos J, Pruitt WO (1977) *Crop water requirements*. FAO irrigation and drainage paper 24. Land and Water Development Division, FAO, Rome, p. 144
- Elgaali E, Garcia LA, Ojima DS (2007) High resolution modeling of the regional impacts of climate change on irrigation water demand. *Clim Chang* 84:441–461. doi:10.1007/s10584-007-9278-8
- Elliott J, Deryng D, Müller C, et al. (2014) Constraints and potentials of future irrigation water availability on agricultural production under climate change. *Proc Natl Acad Sci U S A* 111:3239–3244. doi:10.1073/pnas.1222474110
- Fischer G, Tubiello FN, van Velthuisen H, Wiberg DA (2007) Climate change impacts on irrigation water requirements: effects of mitigation, 1990–2080. *Technol Forecast Soc Chang* 74:1083–1107. doi:10.1016/j.techfore.2006.05.021
- Flato GM (2005) The third generation coupled global climate model (CGCM3). Available on line at <http://www.cccma.bc.ec.gc.ca/models/cgcm3.Shtml>
- Food and Agriculture Organization of the United Nations (FAO) (1999) *The state of food insecurity in the world*. Rome, Italy: FAO.
- Foley JA, Ramankutty N, Brauman KA, et al. (2011) Solutions for a cultivated planet. *Nature* 478:337–342. doi:10.1038/nature10452
- Galin VY, Volodin EM, Smyshlyayev SP (2003) Atmospheric general circulation model of INM RAS with ozone dynamics. *Russ Meteorol Hydrol* 5:13–22
- Garrote L, Iglesias A, Granados A, et al. (2015) Quantitative assessment of climate change vulnerability of irrigation demands in Mediterranean Europe. *Water Resour Manag* 29:325–338. doi:10.1007/s11269-014-0736-6
- Gohari A, Bozorgi A, Madani K, et al. (2014) Adaptation of surface water supply to climate change in Central Iran. *J Water Clim Chang* 5: 391–407
- Gohari A, Eslamian S, Abedi-Koupaei J, et al. (2013) Climate change impacts on crop production in Iran's Zayandeh-Rud River Basin. *Sci Total Environ* 442:405–419. doi:10.1016/j.scitotenv.2012.10.029
- Gondim RS, de Castro MA, Maia ADH, Evangelista SR, Fuck SCDF (2012) Climate change impacts on irrigation water needs in the Jaguaribe River Basin1. *JAWRA J Am Water Resour Assoc* 48: 355–365. doi:10.1111/j.1752-1688.2011.00620.x
- Gordon C, Cooper C, Senior CA, Banks H, Gregory JM, Johns TC, Mitchell JFB, Wood RA (2000) The simulation of SST, sea ice extents and ocean heat transports in a version of the Hadley Centre coupled model without flux adjustments. *Clim Dyn* 16:147–168
- Gordon HB, Rotstayn LD, McGregor JL, Dix MR, Kowalczyk, O'Farrell SP, Waterman LJ, Hirst AC, Wilson SG, Collier MA, Watterson IG ET (2002) The CSIRO Mk3 climate system model. Asoendale CSIRO Atmos Res Tech Pap 130.
- Greasby TA, Sain SR (2011) Multivariate spatial analysis of climate change projections. *J Agric Biol Environ Stat* 16:571–585
- Greene AM, Goddard L, Lall U (2006) Probabilistic multimodel regional temperature change projections. *J Clim* 19:4326–4343
- Guo R, Lin Z, Mo X, Yang C (2010) Responses of crop yield and water use efficiency to climate change in the North China plain. *Agric Water Manag* 97:1185–1194
- Hawkins E, Sutton R (2009) The potential to narrow uncertainty in regional climate predictions. *Bull Am Meteorol Soc* 90:1095–1107
- Hourdin F, Musat I, Bony S, et al. (2006) The LMDZ4 general circulation model: climate performance and sensitivity to parametrized physics with emphasis on tropical convection. *Clim Dyn* 27:787–813. doi:10.1007/s00382-006-0158-0
- Intergovernmental Panel on Climate Change (IPCC) (2007) *General guidelines on the use of scenario data for climate impact and adaptation assessment*. Cambridge and New York: Cambridge University Press.
- Jones PG, Thornton PK (2003) The potential impacts of climate change on maize production in Africa and Latin America in 2055. *Glob Environ Chang* 13:51–59
- Joyce BA, Mehta VK, Purkey DR, et al. (2011) Modifying agricultural water management to adapt to climate change in California's central valley. *Clim Chang* 109:299–316
- Kiehl JT, Hack JJ, Bonan GB, et al. (1998) The national center for atmospheric research community climate model: CCM3. *J Clim* 11: 1131–1178

- Kloster S, Dentener F, Feichter J, et al. (2010) A GCM study of future climate response to aerosol pollution reductions. *Clim Dyn* 34: 1177–1194
- Knox JW, Rodríguez Díaz JA, Nixon DJ, Mkhwanazi M (2010) A preliminary assessment of climate change impacts on sugarcane in Swaziland. *Agric Syst* 103:63–72. doi:10.1016/j.agsy.2009.09.002
- Knutti R, Hegerl GC (2008) The equilibrium sensitivity of the earth's temperature to radiation changes. *Nat Geosci* 1:735–743
- Lee J, De Gryze S, Six J (2011) Effect of climate change on field crop production in California's Central Valley. *Clim Chang* 109:335–353
- Lee J-Y, Wang B (2014) Future change of global monsoon in the CMIP5. *Clim Dyn* 42:101–119
- Lee J-L, Huang W-C (2014) Impact of climate change on the irrigation water requirement in Northern Taiwan. *Water* 6:3339–3361. doi:10.3390/w6113339
- McFarlane NA, Boer GJ, Blanchet J-P, Lazare M (1992) The Canadian Climate Centre second-generation general circulation model and its equilibrium climate. *J Clim* 5:1013–1044. doi:10.1175/1520-0442(1992)005<1013:TCCCSG>2.0.CO;2
- Morid S, Bavani ARM (2010) Exploration of potential adaptation strategies to climate change in the Zayandeh Rud irrigation system, Iran. *Irrig Drain* 59:226–238
- Multsch S, Exbrayat J-F, Kirby M, et al. (2015) Reduction of predictive uncertainty in estimating irrigation water requirement through multi-model ensembles and ensemble averaging. *Geosci Model Dev* 8: 1233–1244. doi:10.5194/gmd-8-1233-2015
- Olesen JE, Bindi M (2002) Consequences of climate change for European agricultural productivity, land use and policy. *Eur J Agron* 16:239–262
- Özdoğan M (2011) Modeling the impacts of climate change on wheat yields in Northwestern Turkey. *Agric Ecosyst Environ* 141:1–12
- Pindyck RS (2012) Uncertain outcomes and climate change policy. *J Environ Econ Manag* 63:289–303. doi:10.1016/j.jeem.2011.12.001
- Postel S (1999) Pillar of sand: can the irrigation miracle last? *Geogr Rev* 89(3):463. doi:10.2307/216168
- Raje D, Mujumdar PP (2010) Reservoir performance under uncertainty in hydrologic impacts of climate change. *Adv Water Resour* 33:312–326
- Rehana S, Mujumdar PP (2013) Regional impacts of climate change on irrigation water demands. *Hydrol Process* 27:2918–2933
- Reilly JM, Schimmelpfennig D (1999) Agricultural impact assessment, vulnerability, and the scope for adaptation. *Clim Chang* 43:745–788. doi:10.1023/A:1005553518621
- Richardson CW, Wright DA (1984) WGEN : a model for generating daily weather variables by. US Department of Agriculture, Agricultural Research Service, Washington, DC
- Riediger J, Breckling B, Svoboda N, Schröder W (2016) Modelling regional variability of irrigation requirements due to climate change in Northern Germany. *Sci Total Environ* 541:329–340. doi:10.1016/j.scitotenv.2015.09.043
- Rodríguez Díaz JA, Weatherhead EK, Knox JW, Camacho E (2007) Climate change impacts on irrigation water requirements in the Guadalquivir river basin in Spain. *Reg Environ Chang* 7:149–159. doi:10.1007/s10113-007-0035-3
- Roeckner E, Bäuml G, Bonaventura L, Brokopf R, Esch M, Giorgetta M, Hagemann S, Kirchner I, Kornbluh L, Manzini E, Rhodin A (2003) The atmospheric general circulation model ECHAM 5. PART I: model description
- Roeckner E, Arpe K, Bengtsson L, Christoph M, Claussen M, Dümenil L, Esch M, Giorgetta M, Schlese U, Schulzweida U (1996) The atmospheric general circulation model ECHAM-4: model description and simulation of present-day climate. MPI Rep 171:218
- Savé R, de Herralde F, Aranda X, et al. (2012) Potential changes in irrigation requirements and phenology of maize, apple trees and alfalfa under global change conditions in Fluvia watershed during XXIst century: results from a modeling approximation to watershed-level water balance. *Agric Water Manag* 114:78–87. doi:10.1016/j.agwat.2012.07.006
- Schmidt GA, Ruedy R, Hansen JE, et al. (2006) Present-day atmospheric simulations using GISS ModelE: comparison to in situ, satellite, and reanalysis data. *J Clim* 19:153–192. doi:10.1175/JCLI3612.1
- Semenov MA (2007) Development of high-resolution UKCIP02-based climate change scenarios in the UK. *Agric For Meteorol* 144:127–138. doi:10.1016/j.agrformet.2007.02.003
- Semenov MA, Barrow EM (2002) A stochastic weather generator for use in climate impact studies. User Manual, Hertfordshire, UK
- Shahid S (2011) Impact of climate change on irrigation water demand of dry season Boro rice in northwest Bangladesh. *Clim Chang* 105: 433–453. doi:10.1007/s10584-010-9895-5
- Shibata K, Yoshimura H, Ohizumi M, et al. (1999) A simulation of troposphere, stratosphere and mesosphere with an MRI/JMA98 GCM. *Pap Meteorol Geophys* 50:15–53
- Smith M (1992) CROPWAT: a computer program for irrigation planning and management (No. 46). Food & Agriculture Org, Rome
- Tebaldi C, Knutti R (2007) The use of the multi-model ensemble in probabilistic climate projections. *Philos Transact A Math Phys Eng Sci* 365:2053–2075
- Teixeira EI, Fischer G, van Velthuisen H, et al. (2013) Global hot-spots of heat stress on agricultural crops due to climate change. *Agric For Meteorol* 170:206–215
- Teutschbein C, Seibert J (2012) Bias correction of regional climate model simulations for hydrological climate-change impact studies: review and evaluation of different methods. *J Hydrol* 456–457:12–29. doi:10.1016/j.jhydrol.2012.05.052
- Trnka M, Olesen JE, Kersebaum KC, et al. (2011) Agroclimatic conditions in Europe under climate change. *Glob Chang Biol* 17:2298–2318. doi:10.1111/j.1365-2486.2011.02396.x
- Valverde P, Serralheiro R, de Carvalho M, et al. (2015) Climate change impacts on irrigated agriculture in the Guadiana river basin (Portugal). *Agric Water Manag* 152:17–30. doi:10.1016/j.agwat.2014.12.012
- UNESCO (2012) Managing Water under Uncertainty and Risk, United Nations Educational, Scientific and Cultural Organization, Paris, France.
- Wada Y, Bierkens MFP (2014) Sustainability of global water use: past reconstruction and future projections. *Environ Res Lett* 9:104003. doi:10.1088/1748-9326/9/10/104003
- Wilby RL, Harris I (2006) A framework for assessing uncertainties in climate change impacts: low-flow scenarios for the River Thames, UK. *Water Resour Res* 42:1–10. doi:10.1029/2005WR004065
- Williams KD, Tselioudis G (2007) GCM intercomparison of global cloud regimes: present-day evaluation and climate change response. *Clim Dyn* 29:231–250
- Woznicki SA, Nejadhashemi AP, Parsinejad M (2015) Climate change and irrigation demand: uncertainty and adaptation. *J Hydrol Reg Stud* 3:247–264. doi:10.1016/j.ejrh.2014.12.003
- Zareian MJ, Eslamian S, Safavi HR (2014) A modified regionalization weighting approach for climate change impact assessment at watershed scale. *Theor Appl Climatol* 122:497–516